

Supporting Information

A size-controlled DNA-cross-linked hydrogel coated silica nanoparticles served as ratio fluorescent probe for the detection of adenosine triphosphate in living cells

Xiaoting Ji, Junning Wang, Shuyan Niu, Caifeng Ding*

**Corresponding author: Key Laboratory of Optic-electric Sensing and Analytical Chemistry for Life Science, Ministry of Education; Shandong Key Laboratory of Biochemical Analysis; Key Laboratory of Analytical Chemistry for Life Science in Universities of Shandong; College of Chemistry and Molecular Engineering, Qingdao University of Science and Technology, Qingdao 266042, PR China. Email: dingcaifeng2003@163.com*

Experiment

Reagents and Instruments. 1-(3-dimethylaminopropyl)-3-ethylcarbodiimide hydrochloride (EDC, $>98\%$), N-hydroxysuccinimide (NHS, $>99\%$), Tris (hydroxymethyl) aminomethane (Tris-base), 2-Hydroxy-4'-(2-hydroxyethoxy)-2-methylpropiophenone (I2959) were purchased from Sigma-Aldrich Co (USA). Sodium chloride (NaCl), Magnesium chloride hexahydrate ($\text{MgCl}_2 \cdot 6\text{H}_2\text{O}$) were purchased from Sinopharm Chemical Reagent Co.,Ltd. Methylpropenoic acid (MA) were purchased from Shanghai Maclean Biochemical Technology Co., Ltd. Amino modified silica nanoparticles (SiNPs) were purchased from Xi'an Ruixi Biological Technology Co., Ltd. RPMI 1640 medium, fetal bovine serum, penicillin/streptomycin were purchased from Thermo Fisher Scientific Co. (USA). Cell Counting Kit-8(CCK-8) was purchased from Shanghai Qihai Futai Biological Technology Co., Ltd. Sequences of the oligonucleotides listed in Table S1 were ordered from Sangon Biotechnology Inc. Adenosine triphosphate (ATP), thymine triphosphate (TTP) and guanosine triphosphate (GTP) were synthesized by Sangon Biotechnology Inc. (Shanghai, China). Liver hepatocellular carcinoma cells (HepG2) were obtained from Jiangsu Keygen Biotech Corp., Ltd (China). All aqueous solution was prepared with ultrapure water produced by Milli-Q.

Transmission electron microscopy (TEM) graphs were performed on a transmission electron microscope (H-7650, Hitach, Japan). The UV-vis absorption spectra were determined by a UV-vis spectrophotometer (UH5300, Hitachi, Japan). Zeta potential and dynamic light scattering (DLS) were performed at 25 °C using a laser particle size distribution analyzer (NanoZS, Malvern, United Kingdom). Confocal laser scanning microscopy (CLSM) images were recorded using a

confocal laser scanning microscope (TCS SP5, Leica, Germany). Fluorescence spectroscopy was monitored by a fluorescence spectrophotometer (F-4500, Hitachi, Japan). CCK-8 assay was recorded by a microplate reader (Bio-tek ELx800, Bio Tek, USA).

Construction of SiNPs-MA-DNA 1 Structure. 10 μL of NHS (4.78×10^{-3} M) was added into 23.5 μL DNA 1 (1×10^{-5} M) and incubated at 25 $^{\circ}\text{C}$ for 30 minutes. while taking 10 μL EDC (1.04×10^{-3} M) was added into 21 μL MA (1.17×10^{-4} M) and incubated at 25 $^{\circ}\text{C}$ for 30 minutes. Then mixing the activated MA with the activated DNA 1, and shaking for 3 min, and then placing it in a 4 $^{\circ}\text{C}$ for 12 h. The product A is obtained. 10 μL of NHS (4.78×10^{-3} M) was added into 10 μL silicon nanoparticles (50 nm) and incubated at 25 $^{\circ}\text{C}$ for 30 minutes, and the product A was added to the activated silicon nanoparticles to continue the reaction, and placed in 4 $^{\circ}\text{C}$ for 12 h to obtain SiNPs-MA-DNA 1 complex.

Construction of MA-DNA 2 Structure. 10 μL of NHS (4.78×10^{-3} M) was added into 52.15 μL DNA 2 (1×10^{-5} M) and incubated at 25 $^{\circ}\text{C}$ for 30 minutes. while taking 10 μL EDC (1.04×10^{-3} M) was added into 4.01 μL methacrylic acid (1.17×10^{-2} M) and incubated at 25 $^{\circ}\text{C}$ for 30 minutes. Then mixing the activated MA with the activated DNA 2, and shaking for 3 min, and then placing it in a 4 $^{\circ}\text{C}$ for 12 h. MA-DNA 2 complex was obtained.

Preparation of SiNPs-PMA-DNA 1. At room temperature, The SiNPs-MA-DNA 1 complex, 10 μL of 1% solution of the initiator I2959, 100 μL of buffer (100 mM Tris-HCl, 500 mM NaCl, 100 mM MgCl_2), and 346.5 μL of water were mixed. The solution was kept under UV irradiation (365 nm) for 30 min. The SiNPs-PMA-DNA 1 was obtained.

Preparation of PMA-DNA 2. At room temperature, product II, 4 μL of 1% solution of the initiator I2959, 20 μL of buffer (100 mM Tris-HCl, 500 mM NaCl, 100 mM MgCl_2), and 119.85 μL of water were mixed together. The Solution was irradiated with UV light for 30 min.

Synthesis of DNA-cross-linked SiNPs nanohydrogel. At room temperature, 100 μL of SiNPs-PMA-DNA 1 solution, 19.58 μL of PMA-DNA 2 solution, and 4.7 μL of 1×10^{-5} M ATP aptamer were mixed together and kept in a water bath at 95°C for 5 min, followed by slow cooling to room temperature.

Cell culture. The HepG2 cells were cultured in a RPMI 1640 medium at 37°C under 5% CO_2 atmosphere, completed with 1% penicillin-streptomycin and 10% FBS. The medium was replaced every day, and the cells were digested with trypsin before further used.

CCK-8 Assay. The CCK-8 assay was adopted to study the cytotoxicity of the nanoprobe. Briefly, HepG2 cells (8×10^3 cells/well) were dispersed within replicate 96-well microtiter plates to a total volume of 200 μL well⁻¹ and were incubated at 37°C in a 5% CO_2 incubator for 24 h. Then the original medium was removed, and the HepG2 cells were incubated with fresh medium containing nanoprobe (100 nM) for 1, 3, 5, 7 and 9 h. Ultimately, the cells were washed with $1 \times$ PBS for three times and 10 μL CCK-8 solutions were added into each well. After incubation for 1-2 h, the absorbance was measured at 450 nm with a bioTek microplate reader.

In vitro cell uptake and imaging. The cellular uptake behavior of PTX-LNA and PTX-LNA-TAT in HeLa cells were investigated on the CLSM. A density of 1.0×10^5 HepG2 cells per well were seeded into 16-well plate and incubated with RPMI 1640 medium in an atmosphere containing 5% CO_2 at 37°C for 24 h. The mixture washed three times after incubation for

different time. The PTX-FITC and FAM signal were recorded by fluorescence microscopy at excitation of 488 nm and the emitted light at 520 nm and 565 nm was collected.

Table S1. The sequences of the nucleic acid.

Name	Sequence (5'-3')
DNA 1	CCT TCC TCC TTT T, carboxyfluorescein (FAM) at the 5' terminus, amino at the 3' terminus
DNA 2	GCA ATA CTC CCC TTT T, cyanine-3 (Cy3) at the 5' terminus, amino at the 3' terminus
ATP aptamer	CAC CTG GGG GAG TAT TGC GGA GGA AGG TTT TTT

Results and Discussion

The characterization of infrared spectra (IR) of SiNPs and nanohydrogel. FTIR spectra of amino modified SiNPs and DHSN nanohydrogel are given in Fig. S1. Compare with the FTIR of SiNPs, the absorbance bands at 1635 cm^{-1} and 1530 cm^{-1} , the stretching vibration of carbonyl from the amide bond (amide I band) and inplane bending vibration of N-H (amide II band) respectively revealed the existence of amide which was introduced from DHSN. The characteristic absorbance peak for the $-\text{C}=\text{C}-\text{H}$ units introduced by polymethylacrylic acid were observed at 1188 cm^{-1} and 998 cm^{-1} . The results proved that the nanohydrogel was constructed as expect.

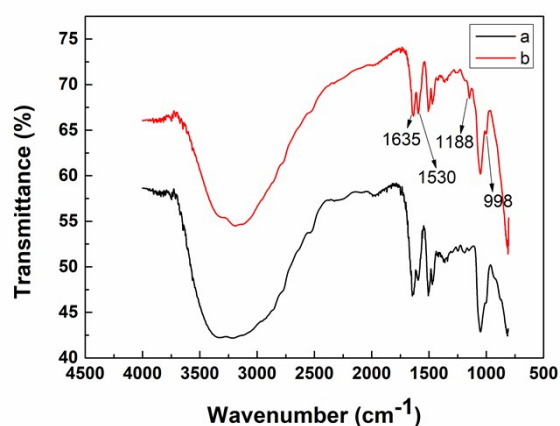


Fig. S1 FTIR spectra of (a) amino modified SiNPs and (b) DHSN nanohydrogel.

The thermogravimetric analysis (TGA) of SiNPs and DHSN. As shown in Fig.S2, DHSN showed the initial weight loss of about 13 wt% at 100 °C due to evaporation of the absorbed humidity. The next step weight loss of about 71 wt% at 150-270 °C. This weight loss can be related to decomposition of highly branched macromolecule consisting of water-soluble fraction and insoluble fraction. In case of SiNPs, only weight loss temperature is observed at 150 °C. The stage loss of ~83 wt% at 150 °C is due to decomposition of SiNPs. These results proved that the nanohydrogel was constructed successfully.

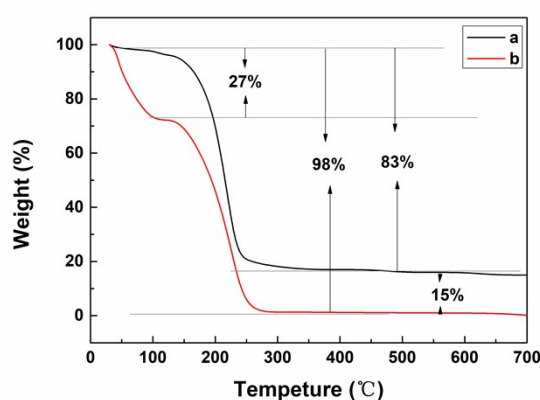


Fig. S2 TGA curves of SiNPs (a) and DHSN (b) nanohydrogel.

The detection feasibility of strategy. The feasibility of the developed strategy for target substance is validated FRET-on or FRET-off. To confirm the obtained fluorescence spectra in the present nanoprobe was depend on amount of ATP, control experiments were done. The result was shown in Fig. S3. The fluorescence signals variation of FAM and Cy3 were monitored in vitro before (curve a) and after (curve b) addition of the target ATP, and the fluorescence intensity of FAM increased around 2.93-fold in the presence of 110 nM ATP, inversely, the fluorescence intensity of Cy3 decreased around 1.62-fold.

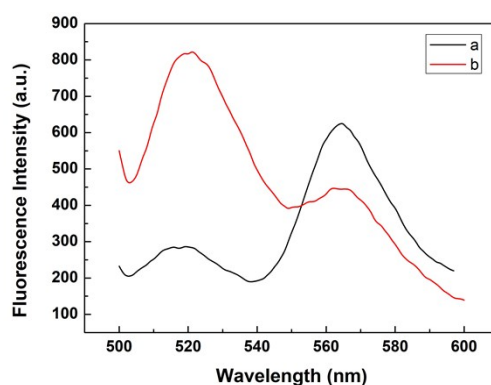


Fig. S3 Fluorescence intensities of DHSN in the presence of 110 nM ATP (curve b) and blank (curve a).

The optimization of reaction condition. To obtain the best ratio performance of fluorescent intensity activity assay, confirming the ratio of MA and DNA, reaction temperature and reaction temperature are necessary. Fig. S4A showed that the intensities of fluorescent ratio increased rapidly upon the ratio of MA and DNA 1 from 0 to 1.7, and then when the ratio exceeded 1.7, the fluorescent intensity tended to constant. Thus, the ratio of MA and DNA 1 of 1.7 was used all through the assays. Similarly, Fig. S4B showed that the ratio of fluorescent intensity increased rapidly upon the ratio of MA and DNA 2 from 0 to 100, and then when the ratio exceeded 100, the fluorescent intensity tended to constant. Thus, the ratio of MA and DNA 2 of 100 was used all

through the assays. Besides, Fig. S4C showed that the ratio of fluorescent intensity increased rapidly upon the release time from 0.5 h to 1.5 h, and then when the release time exceeded 1.5 h, the fluorescent ratio tended to reduce. Thus, the release time of 1.5 h was used all through the assays. In addition, Fig. S4D showed that the ratio of fluorescent intensity increased upon the reaction temperature from 20 °C to 25 °C, and then when the reaction temperature exceeded 25 °C, the fluorescent ratio tended to reduce. Thus, the reaction temperature of 25 °C was used all through the assays.

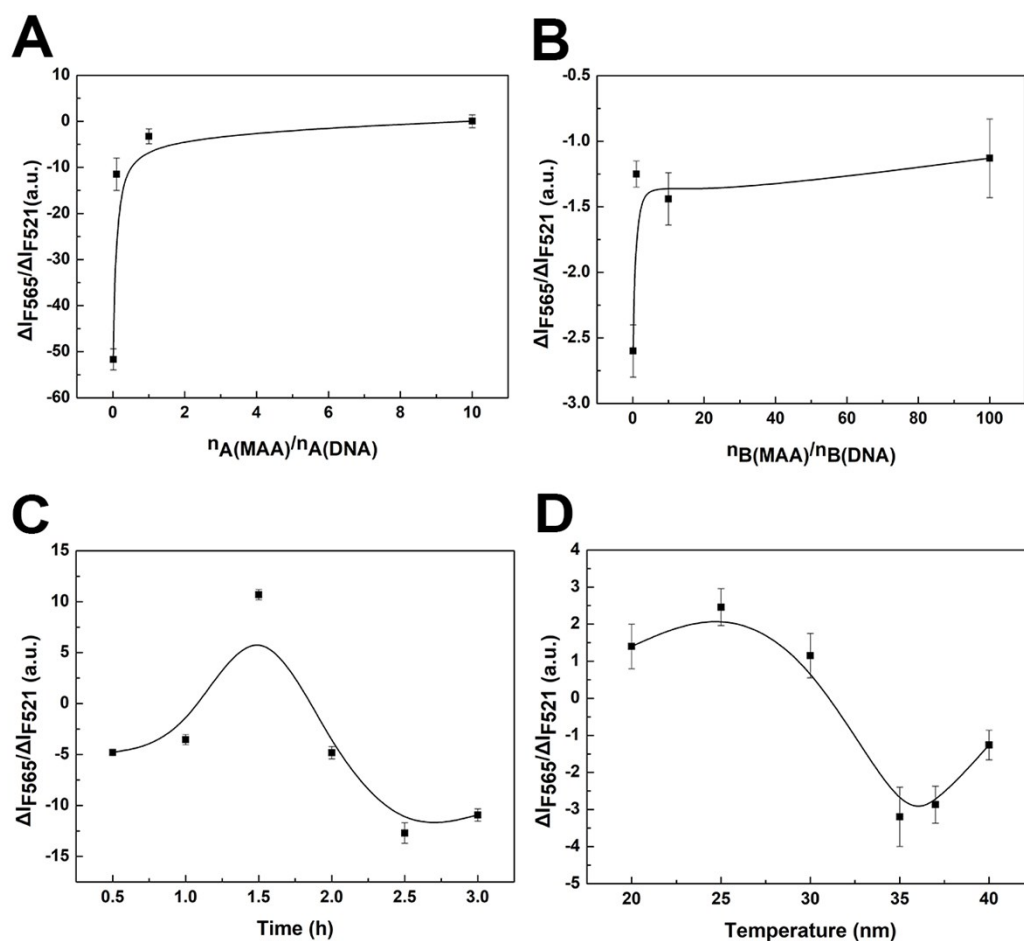


Fig. S4 The optimization of reaction condition. (A) The optimization of ratio of MA and DNA 1. (B) The optimization of ratio of MA and DNA 2. (C) The optimization of reaction time. (D) The optimization of reaction temperature.

The optimization of pH in presence of target ATP. To obtain the best ratio performance of fluorescent intensity activity assay, confirming pH is necessary. As the Fig. S5 showed, the ratio of fluorescent intensity was influenced by pH. When the pH of 6.5 was reaction condition, the ratio of fluorescent intensity had obvious performance. What's more, because the pH of 6.5 is important characteristic in cancer cells, the nanoprobe is suitable for sensing target ATP in cells.

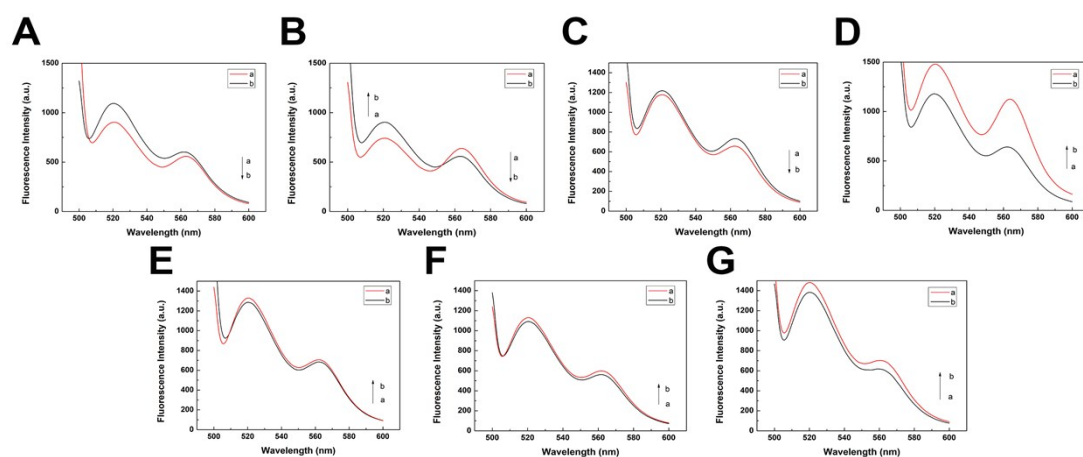


Fig. S5 The optimization of reaction condition of pH. (A: pH 5.5, B: pH 6.0, C: pH 6.5, D: pH 7.0; E: pH 7.4, F: pH 8.0, G: pH 8.5; fluorescence emission spectra of assay with different sample. a: blank, b: 60 nM ATP)

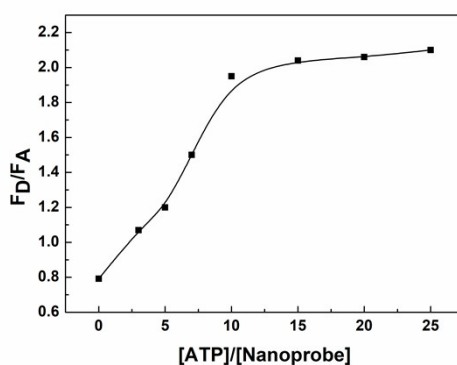


Fig. S6 (A). Fluorescence intensity ratios to different the ratio of ATP and DHSN.

The stoichiometric analysis of ATP and DHSN. To determine the maximum number of DHSN bound with ATP, stoichiometric analysis was constructed by using the fluorescence intensity ratio as a function of the molar fraction of DHSN in Tris-HCl (pH 6.5). As shown in Fig. S6, the ratio

of fluorescent intensity increased rapidly upon the molar ratio of ATP and DHSN from 0 to 10, and then when the ratio exceeded 10, the fluorescent intensity ratio tended to constant, suggesting that the formation of the DHSN-ATP complex followed a 1:10 stoichiometry.

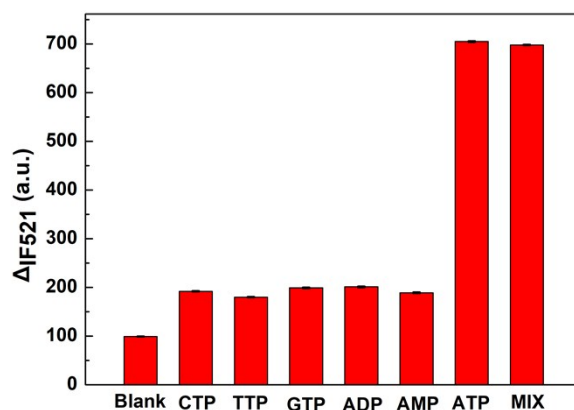


Fig. S7 The intensity of fluorescence to diverse bioanalytes in PBS. (the concentration of ATP was 80 nM; the concentration of CTP, GTP, TTP, AMP, ADP, A were 80 μ M).

The stability studies of PTX-LNA-TAT nanomicelle. In order to confirm the stability of DHSN nanoprobe, DHSN nanoprobe stored from 1 day to 7 day were evaluated by fluorescence spectroscopy assay. 40 nM, 60 nM, 80 nM ATP and nanoprobe were incubated at 25 $^{\circ}$ C for 1.5 h, the ratio of fluorescent intensities are constant at 1.4, 1.5, 1.8 (Fig. S8). These results indicate that the nanoprobe has high stability and easy to store.

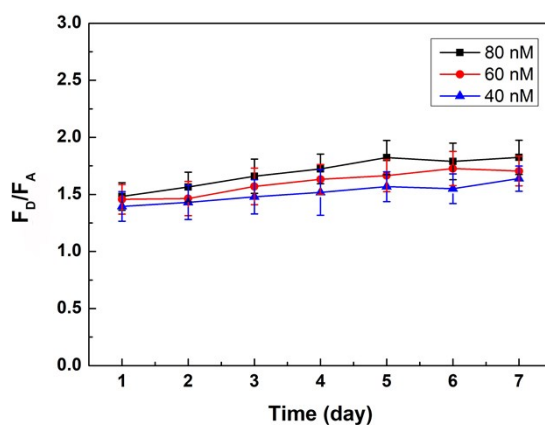


Fig. S8 The stability of nanoprobe.

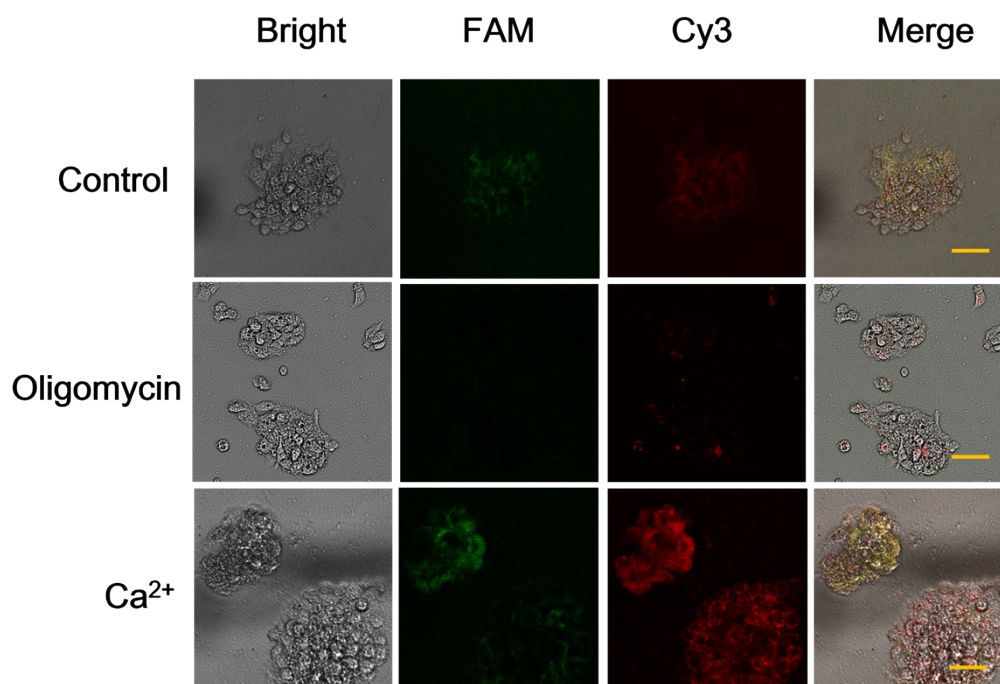


Fig. S9 Fluorescence images of HepG2 cells treated with medium (top), 10 μ M oligomycin (middle), and 5 mM Ca^{2+} (bottom), followed by incubation with 10 μ M DHSN for 3 h at 37 $^{\circ}$ C. Scale bars: 10 μ m.